

Interference effects on Higgs mass measurement at CEPC

Zhang Yu-Jie¹

nophy0@gmail.com ¹School of Physics, Beihang University

Coauthor: Gang Li, Yi-Jie Li, Kui-Yong Liu, and Guang-Zhi Xu

Base on arXiv:1505.06981, 160X.XXXXX

Proposal discussions in light of the CEPC CDR preparation
Dec. 14, 2015, IHEP

Outline

- 1 Introduction**
 - New Physics is Necessary
 - New Accelerator is Necessary
 - CEPC as a Higgs Factory
- 2 Calculation frame**
 - Feynman Amplitude
- 3 Result of $ZH(\gamma\gamma)$**
 - Input Parameters
 - Result
- 4 Result of $Z(\mu^+\mu^-)H(b\bar{b})$**
 - Input Parameters
 - Numerical Result
- 5 Summary and Outlook**

Introduction

New Physics is Necessary

The discovery of Higgs at LHC is not the end of particle physics but a new starting point.

Theoretical aspect

Contains only strong, weak and electromagnetic interactions, but no gravity. It is failed at the Planck scale.

Experimental aspect

The asymmetry between matter and antimatter in the universe. Dark matter, dark energy.

Aesthetics aspect

More than 26 basic parameters, miscellaneous!

Higgs is Important in NP

Precise test of SM

- Yukawa coupling
- 3 Higgs coupling
- 4 Higgs coupling

Vacuum

- Vacuum Structure and Stability
- Vacuum Energy and Dark Energy

Cosmology

- CP Violation: Baryogenesis, Leptogenesis
- Scalar Dark Matter from Higgs sector?

New Accelerator is Necessary

Future e^+e^- colliders

- International Linear Collider (ILC),
- Triple-Large Electron-Positron Collider (FCC-ee),
- **Circular Electron Positron Collider (CEPC)**,
- ...

Future hadron colliders

- Future Circular Collider (FCC),
- **Super Proton-Proton Collider (SPPC)**,
- ...

CEPC as a Higgs Factory

ΔM_H	Γ_H	$\sigma(ZH)$	$\sigma(\nu\bar{\nu}H) \times \text{BR}(H \rightarrow b\bar{b})$
5.9 MeV	2.8%	0.51%	2.8%

Decay mode	$\sigma(ZH) \times \text{BR}$	BR
$H \rightarrow b\bar{b}$	0.28%	0.57%
$H \rightarrow c\bar{c}$	2.2%	2.3%
$H \rightarrow gg$	1.6%	1.7%
$H \rightarrow \tau\tau$	1.2%	1.3%
$H \rightarrow WW$	1.5%	1.6%
$H \rightarrow ZZ$	4.3%	4.3%
$H \rightarrow \gamma\gamma$	9.0%	9.0%
$H \rightarrow \mu\mu$	17%	17%
$H \rightarrow \text{inv}$	—	0.28%

Figure: Estimated precisions of Higgs boson measurements at the CEPC, From CEPC-preCDR

Diphoton invariant mass distributions

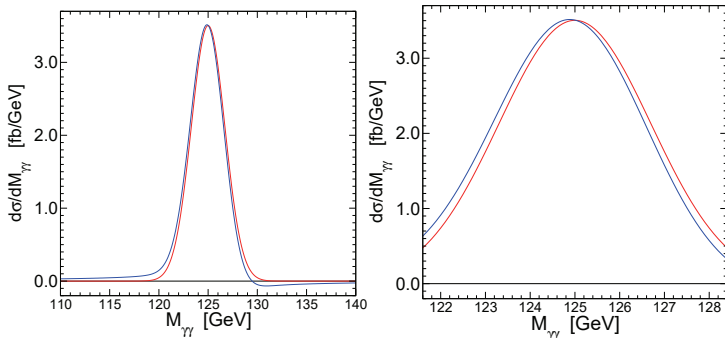


Figure: Diphoton invariant mass distributions in $gg \rightarrow \gamma\gamma$ with a Gaussian mass resolution of width $\sigma_{MR} = 1.7$ GeV., from 1208.1533

The interference peak related with Higgs mass and width

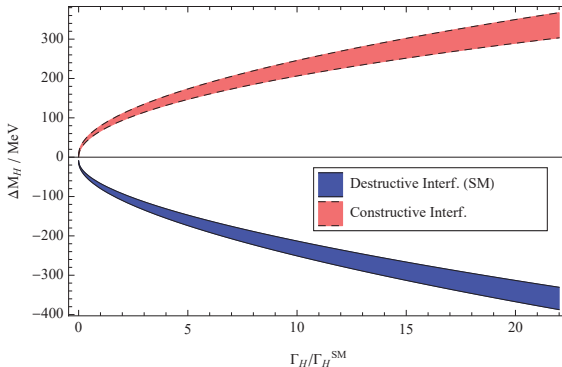


Figure: The peak related with Higgs mass, width, and signal-background interference in $gg \rightarrow \gamma\gamma$. Higgs mass shift as a function of the Higgs width, from 1305.3854

Signal-background interference move the peak

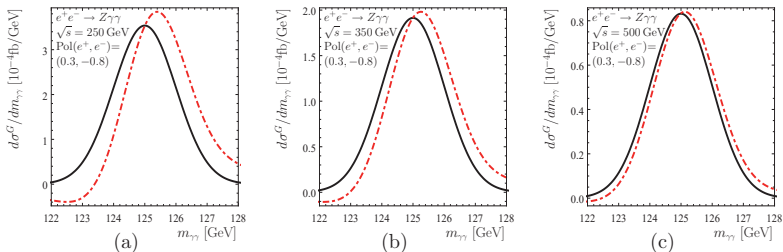


Figure 8: Smearred $d\sigma_S^G/dm_{\gamma\gamma}$ (black, solid) and $d\sigma_{S+I}^G/dm_{\gamma\gamma}$ (red, dot-dashed) in fb/GeV as a function of $m_{\gamma\gamma}$ in GeV for $e^+e^- \rightarrow Z\gamma\gamma$ with $\hat{\sigma} = 1$ GeV for (a-c) $\sqrt{s} = 250, 350, 500$ GeV.

Figure: Signal-background interference move the peak, from 1503.07830

Calculation frame

The typical Feynman diagrams of $ZH(\gamma\gamma)$

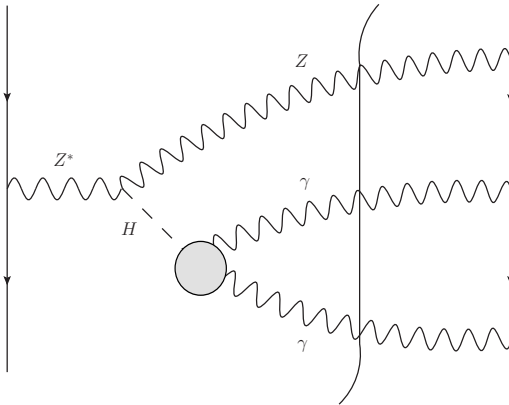


Figure: The typical Feynman diagrams of signal-background interference

Feynman Amplitude

With the narrow-width approximation, the pure signal and interference cross sections for the production can be expressed as:

$$\begin{aligned} \frac{d\sigma^{bac}}{dM_{\gamma\gamma}} &= |\mathcal{A}_{e^+e^- \rightarrow Z\gamma\gamma}|^2, \\ \frac{d\sigma^{sig}}{dM_{\gamma\gamma}} &= \left| \mathcal{A}_{e^+e^- \rightarrow ZH} \frac{i}{(m_{\gamma\gamma}^2 - m_H^2) + im_H\Gamma_H} \mathcal{A}_{H \rightarrow \gamma\gamma} \right|^2, \\ \frac{d\sigma^{ex}}{dM_{\gamma\gamma}} &= \left| \mathcal{A}_{e^+e^- \rightarrow Z\gamma\gamma} + \right. \\ &\quad \left. \mathcal{A}_{e^+e^- \rightarrow ZH} \frac{i}{(m_{\gamma\gamma}^2 - m_H^2) + im_H\Gamma_H} \mathcal{A}_{H \rightarrow \gamma\gamma} \right|^2, \quad (1) \end{aligned}$$

Higher order corrections of $\mathcal{A}_{H\rightarrow\gamma\gamma}$

- The three- and four-loop $\mathcal{A}_{H\rightarrow\gamma\gamma}$ has been calculated [1, 2], which contributions can be neglected.
- For the two-loop QCD and electroweak corrections are nearly completely cancelled for $m_H \sim 125$ GeV.

Amplitude [3]

$$\mathcal{A}_{H\rightarrow\gamma\gamma} = \frac{i\sqrt{\sqrt{2}G_F}}{4\pi} m_{\gamma\gamma}^2 \left[F_1(4m_W^2/m_{\gamma\gamma}^2) + \sum_{f=t,b,c,\tau} N_f e_f^2 F_{1/2}(4m_f^2/m_{\gamma\gamma}^2) \right] \quad (2)$$

Higher order corrections of $e^+e^- \rightarrow ZH$ and $e^+e^- \rightarrow Z\gamma\gamma$

Higher order corrections of $e^+e^- \rightarrow ZH$

- The electroweak radiative correction was calculated [4, 5].
- The contribution is less than 5% for a Higgs with mass of 125 GeV[6].

$e^+e^- \rightarrow Z\gamma\gamma$

- The NLO electroweak corrections is about 2.32% [7].

Ignore higher order corrections

- LO $e^+e^- \rightarrow ZH$.
- LO $e^+e^- \rightarrow Z\gamma\gamma$.
- One Loop level $H \rightarrow \gamma\gamma$.

Smearing effect

Smearing effect

- The finite experimental resolution smear the peak. [3].
- Smeared distribution

$$\frac{d\sigma}{dM_{\gamma\gamma}} = \int dM \left(\frac{d\sigma}{dM} \right) \frac{1}{\sigma_{MR}\sqrt{2\pi}} \exp \left[-\frac{(M_{\gamma\gamma} - M)^2}{2\sigma_{MR}^2} \right]. \quad (3)$$

- The the measured mass is

$$\langle M_{\gamma\gamma} \rangle = \frac{\int dM_{\gamma\gamma} M_{\gamma\gamma} \left(\frac{d\sigma}{dM_{\gamma\gamma}} \right)}{\int dM_{\gamma\gamma} \left(\frac{d\sigma}{dM_{\gamma\gamma}} \right)} \quad (4)$$

- The the mass shift is

$$\Delta M_{\gamma\gamma} = \langle M_{\gamma\gamma} \rangle - M_H \quad (5)$$

Result of $Z + H(\gamma\gamma)$

Input Parameters

The running fermion masses

$$m_t = 168.2 \text{ GeV},$$

$$m_b = 2.78 \text{ GeV},$$

$$m_c = 0.72 \text{ GeV},$$

$$m_\tau = 1.744 \text{ GeV}.$$

Parameters

$$M_H = 125.6 \text{ GeV},$$

$$\Gamma_H = 4.2 \text{ MeV},$$

$$\alpha = 1/137,$$

$$\sqrt{s} = 246 \text{ GeV}$$

Smearing effect and cut

Smearing effect

- The finite experimental resolution smear the peak.
- Convolution integrals with a Gaussian function were added to the cross section to simulate the smearing effect here [3].
- The Gaussian width as $\sigma_{MR} = 0.8, 1.0, 1.5, \text{ or } 2.0 \text{ GeV}$

Cut

- $|\cos \theta_\gamma| < 0.8, |\cos \theta_\gamma| < 0.9, \text{ or } |\cos \theta_\gamma| < 0.95.$
- The cut of the final photon energy is $E_\gamma > 20 \text{ GeV}.$

Result

Background and signal process with different cut.

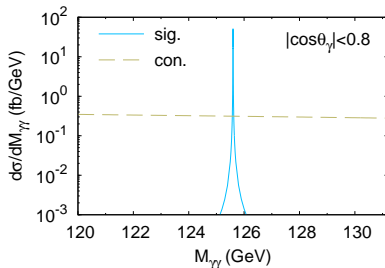
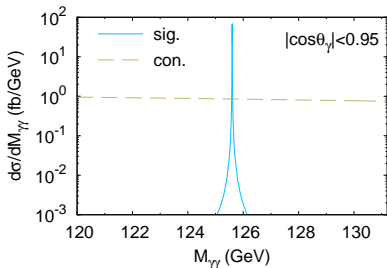


Figure: Comparison of background and signal process with different cut conditions for the final photons.

Result

The diphoton invariant mass distribution

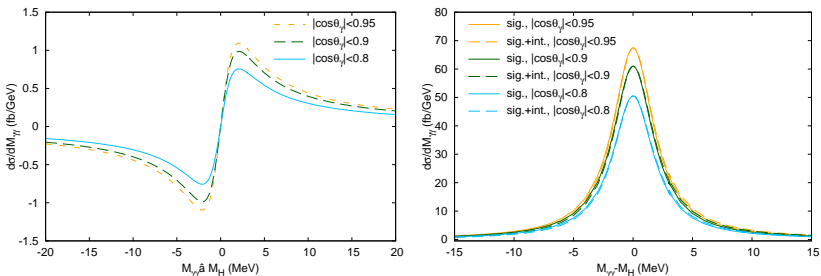


Figure: (a) the diphoton invariant mass distribution from the real interference and (b) the signal with and without interference from the background.

Result

The diphoton invariant mass distribution

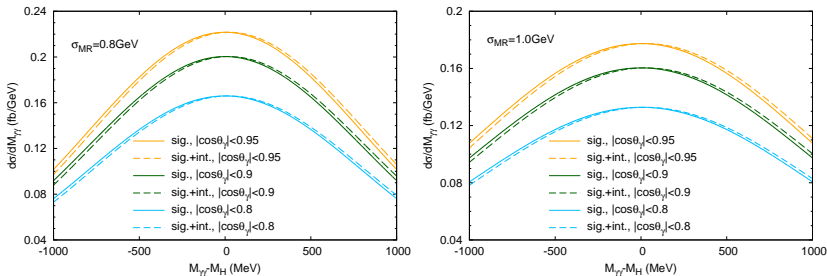


Figure: Diphoton invariant mass distributions of Higgs signal with different mass resolutions and kinematic cuts.

Result

The diphoton invariant mass distribution

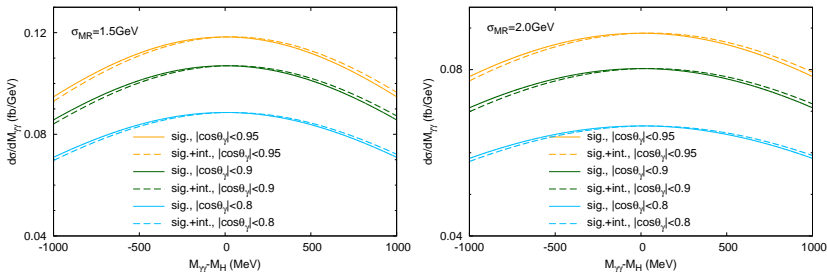


Figure: Diphoton invariant mass distributions of Higgs signal with different mass resolutions and kinematic cuts.

The Higgs mass shifts

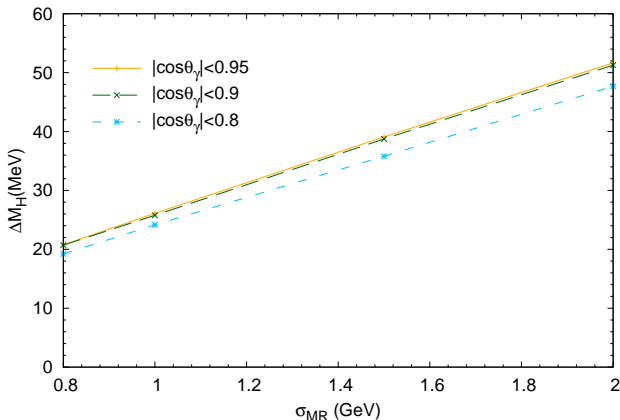


Figure: The Higgs mass shifts due to the signal-background interference as a function of the Gaussian mass resolution width.

Result of $Z(\mu^+\mu^-) + H(b\bar{b})$

The typical Feynman diagrams of $Z(\mu^+\mu^-)H(b\bar{b})$

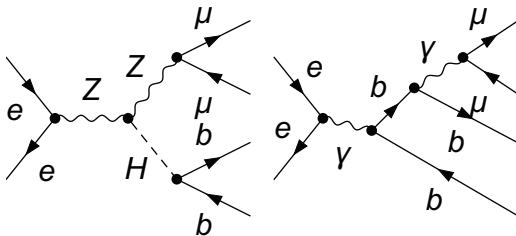


Figure: The typical Feynman diagrams of signal-background interference

Input Parameters

Mass and width

$$m_b = 2.9 \text{ GeV}, \quad \alpha = 1/137,$$

$$M_H = 125.7 \text{ GeV}, \quad \Gamma_H = 4.2 \text{ MeV},$$

$$M_Z = 91.1876 \text{ GeV}, \quad \Gamma_Z = 2.4952 \text{ GeV},$$

$$\sqrt{s} = 250 \text{ GeV}.$$

Parameters

$$y_{b\bar{b}} = \frac{M_{b\bar{b}}^2}{s},$$

$$y_{\mu^+\mu^-} = \frac{M_{\mu^+\mu^-}^2}{s}. \quad (6)$$

Numerical Result

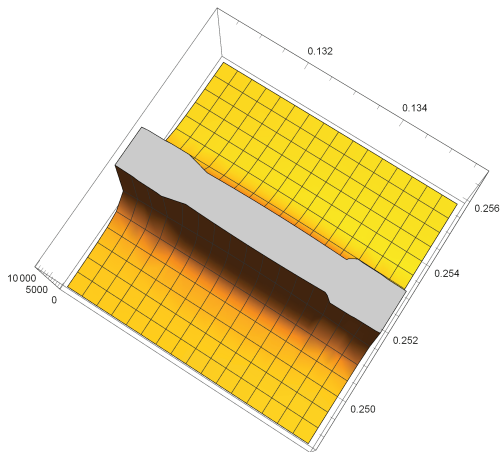
Resonance Distribution on $y_{b\bar{b}}$ and $y_{\mu^+\mu^-}$.

Figure: Resonance Distribution on $y_{b\bar{b}}$ and $y_{\mu^+\mu^-}$.

Numerical Result

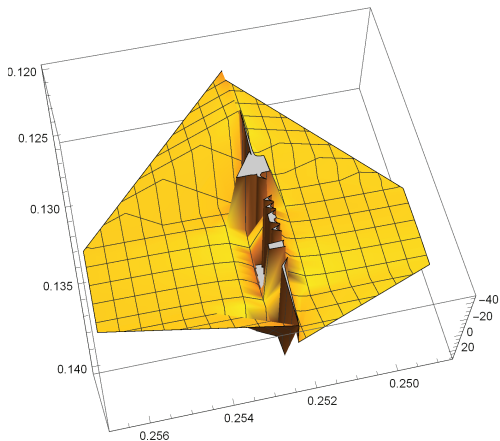
Interference Distribution on $y_{b\bar{b}}$ and $y_{\mu^+\mu^-}$.

Figure: Interference Distribution on $y_{b\bar{b}}$ and $y_{\mu^+\mu^-}$.

Summary and Outlook

Summary and Outlook

Summary

- The smearing Gaussian width σ_{MR} (which simulated the experimental mass resolution) ranging from 0.8 GeV to 2 GeV,
- The corresponding mass shifts of $ZH(\gamma\gamma)$ final state is about **20 MeV to 50 MeV**.

Outlook

- NLO EW corrections @ $e^+e^- \rightarrow ZH(\gamma\gamma)$,
- $e^+e^- \rightarrow Z(\mu^+\mu^-)H(\gamma\gamma)$,
- $e^+e^- \rightarrow Z(\mu^+\mu^-)H(\tau^+\tau^-)$,
- NLO QCD @ $e^+e^- \rightarrow Z(\mu^+\mu^-)H(b\bar{b})$,
- ...

-  Maierhofer and Marquard(2013).
-  Sturm(2014).
-  Martin(2012).
-  Denner,Kniehl, and Kublbeck(1992).
-  Denner,Kublbeck,Mertig, and Bohm(1992).
-  Englert and McCullough(2013).
-  Yu,Lei,Wen-Gan,Ren-You,Chong, et al.(2014).